Preprints (www.preprints.org) | NOT PEER-REVIEWED | Posted: 8 January 2020 doi:10.20944/preprints202001.0061.v1

Peer-reviewed version available at J. Mar. Sci. Eng. 2020, 8, 133; doi:10.3390/jmse8020133

Article

Reflection Analysis of Impermeable Slopes under Bimodal Sea Conditions

Stephen Orimoloye, Harshinie Karunarathna and Dominic E. Reeve *

[1] Energy & Environment Research Group, Zienkiewicz Centre for Computational Engineering, Swansea University, Swansea, SA1 8EN, United Kingdom.

* Correspondence: d.e.reeve@swansea.ac.uk

Abstract: Understanding of reflection characteristics of coastal seawalls is crucial for design. Wave reflection can cause difficulties to small vessel manoeuvring at the harbour entrance and constitute damaging scouring at the toe of coastal structures. Previous studies have considered reflection characteristics of coastal seawalls under wind-generated random waves without paying attention to the effects of wave bimodality created by the presence of swell waves. The present study focuses on the influence of random wave bimodality on reflective characteristics of coastal seawalls. More than eight hundred experimental tests have been conducted to examine the reflection performance of impermeable sloping seawalls under bimodal waves. Reflection coefficients were computed from each test. Analysis of results suggests that both unimodal and bimodal waves give similar reflection characteristics. However, the reflection coefficient in bimodal sea states seems to be more prolonged than in the unimodal sea states. It was found that the reflection coefficient of coastal seawalls is strongly influenced by the seawall slope, the wave steepness, relative water depth, and the surf similarity parameters. A new empirical reflection equation to describe the influence of wave bimodality on the reflection characteristics of coastal seawalls has been formulated based on this study.

Keywords: coastal seawall; impermeable; bimodal seas; reflection coefficient; bimodality; wave steepness; swell percentages

---

1. Introduction

Waves incident on coastal seawalls will be partially reflected unless fully absorbed by the structure. The reflected wave component will interact with the incoming wave creating interference. This can lead to wave amplification, wave breaking, and standing waves Lykke-Anderson [1]. In the case of vertical walls, standing waves can be pronounced Zanuttigh and van der Meer [2]. Standing waves lead to an amplification of wave-induced velocities which can lead to exacerbated scouring of sediments near the toe of the structure, and eventually to the failure and collapse. At locations exposed to local storm waves and open oceans, long period swell waves can be present leading to bimodal wave conditions. Existing literature provides little guidance on reflection characteristics in this situation, which Hawkes et al., [3] considers might constitute the worse-case in terms of wave conditions. Recent studies Thompson et. al., Poliodoro et al. [4,5] provide evidence that bimodal wave conditions constitute worse conditions than pure wind wave conditions of similar total energy content. There remaining a gap in our understanding of seawall performance under bimodal wave conditions. In this paper we present the results of laboratory experiments of bimodal waves impinging an impermeable seawalls.

Previous studies include those of Miche, Ursell and Battjes [6–8]. Miche [6] proposed the reflection coefficient of monochromatic waves on a plane beach. Miche's hypothesis was reformulated by Battjes

Preprints (www.preprints.org) | NOT PEER-REVIEWED | Posted: 8 January 2020 doi:10.20944/preprints202001.0061.v1

Peer-reviewed version available at J. Mar. Sci. Eng. 2020, 8, 133; doi:10.3390/jmse8020133

[8] in terms of waves breaker parameter index after an earlier study conducted by Iribarren [9]. As pointed out by Zanuttigh and van der Meer[2], both studies from Miche and Ursell [7,8] indicated overestimation of reflection coefficient criterion recorded by Miche's [6] formulations. One main advantage of Zanuttigh and van der Meer [2]'s results is the fact large reflection datasets covering several structures are adopted in the study. The prediction formulae from the study apply to both breaking and non-breaking waves. The formulation is also valid for breaker parameters between 1 and 4.1 and for wall slopes of cot α between 1.5 and 4.0. Studies by Battjes [8] and Seelig & Ahrens [10] are limited to breaker parameters less than 2.3 due to the limitations of their laboratory studies.

Some other notable studies were described in Numata, Losada and Gimenez-Curto [11,12]. Numata [11] presented reflection and transmission performances of artificial blocks in a dimensionless form by comparing the ratio of breakwater width to the diameter of the armour. In Losada and Gimenez-Curto [12], flow behaviours created by reflection and transmission were represented in an exponential form. Well-defined interaction curves obtained from wave heights and periods of regular waves were applied to obtain probabilistic standards which serve as input to predict flow patterns of equivalent irregular wave actions. The exponential probability model proposed by Losada and Gimenez-Curto [12] were validated using experimental datasets. Other notable studies include, [13–15], in which reflection performances of different rock slopes and rock armours were presented. Postma [13] investigated rock slopes under irregular wave attack which showed a greater dependence of the reflection coefficient K_r on the breaker index ξ. However, a weaker correlation was obtained in the relationship between K_r with spectral characteristics and depth at the structure toe.

Relationships between K_r and ξ were later improved by Van der Meer [16] by applying a multiple regression analysis combining influences of the characteristics of waves (in terms of heights and periods), and the structure (slope and permeability). Similarly, a modified version of the study by Seelig and Ahrens [10] was presented by Allsop and Hettiarachi [17]. Here values of wave steepness from 0.043 to 0.042 were investigated, which corresponds to ideal wind-sea states. Lower wave steepness which correspond to swell-driven sea conditions under bimodal wave conditions have not been considered. Newer coefficients values for predicting reflection performances of random waves were derived. A more recent study was presented in Neelamani & Sandya [18]. Predictive equations were proposed based on a series of experimental tests derived from wave reflection measurements of several wave heights and wave periods. Different seawall types including plane, dentated and serrated and one water depth were used in all measurements obtained.

Here we investigate values of wave steepness from 0.043 to 0.042, which corresponds to ideal wind-sea states. Lower wave steepness would correspond to swell driven sea conditions under bimodal wave conditions. As observed in some previous studies including Thompson et. al., Poliodoro et al., Orimoloye et. al., [4,5,19], bimodality in sea waves generally increase the wavelength of the wave train. It would, in turn, reduced the wave steepness and could usually alter the breaker parameter indices. These occurrences have not yet been fully investigated for bimodal sea cases. In this paper, both numerical and physical model tests were performed on three different seawalls to examine reflection performances under bimodal wave scenarios. Unimodal and bimodal cases were compared with previously formulated formulas. A new prediction formula which considers reflection coefficients under wave bimodality is proposed. The paper is divided into five sections, the following section (Section 2) briefly explains the formulation of the analytical energy-conserved bimodal spectrum. Section 3 details the numerical modelling of the discretised waves, Sections 4 presents and discuss the results, and the conclusions are presented in Section 5.

Preprints (www.preprints.org) | NOT PEER-REVIEWED | Posted: 8 January 2020 doi:10.20944/preprints202001.0061.v1

Peer-reviewed version available at J. Mar. Sci. Eng. 2020, 8, 133; doi:10.3390/jmse8020133

2. Reflection Characteristics of Smooth Impermeable Slopes

Battjes [8] identified the surf similarity parameter ξ as a critical parameter affecting the reflection characteristics of sloping impermeable slopes with slope angle α under incident monochromatic waves. It can be expressed mathematically as:

$$\xi = \frac{tan\,\alpha}{\sqrt{2\pi H/gT^2}} \tag{1}$$

In this equation, H, and T represent the significant wave height and the wave period of the monochromatic wave, respectively. Values of $\xi \leq 2.3$ are correspond to breaking waves while for $\xi \geq 2.3$ non-breaking waves occur. The equation showing a simplified relationship between the reflection coefficient K_r and the breaker parameter ξ of breaking monochromatic waves has also been described in the same study (Battjes [8]), and is:

$$K_r = 0.1\,\xi^2 \tag{2}$$

This expression is only valid for breaking monochromatic waves $\xi \leq 2.3$ as illustrated by Figure 1. In Seelig and Ahrens [10], a modified version of Equation (2) has been presented. The modified relationship between the reflection coefficient K_r and the breaker parameter xi is presented in Equation (3):

$$K_r = tanh\left(0.1\xi^2\right) \tag{3}$$

It is worth noting that Equation (2) is a close approximation to Equation (3) for small values of the surf similarity parameter. For larger values of the parameter, Equation (3) tends asymptotically to 1. The mathematical expression from Seelig and Ahrens [10] is valid for both breaking and non-breaking monochromatic waves.

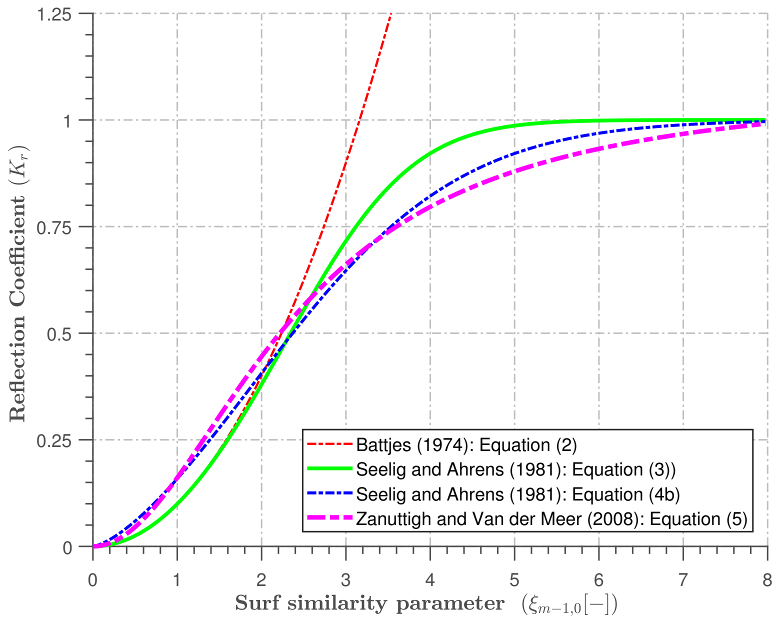

Figure 1. *An illustration of the prediction of reflection characteristics of smooth impermeable slopes*

A more accurate expression was also proposed based on several experimental studies that were performed to describe the reflection behaviour of other sea defences, including revetments, beaches and breakwater. These expressions consider both the peak period of irregular waves and the spectrally determined breaker parameter $\xi_{m-1,0}$. These are described in Equation (4a and 4b) below:

$$K_r = \frac{\xi_p^2}{\xi_p^2 + 5.5} \tag{4a}$$

$$K_r = \frac{\xi_{m-1,0}^2}{\xi_{m-1,0}^2 + 5.0} \tag{4b}$$

Equation (4b) is valid for $1.0 \leq \xi_{m-1,0} \leq 6.2$ and sloping seawalls with $1.5 \leq \cot\alpha \leq 2.5$ respectively.

Zanuttigh and van der Meer [2] proposed a revised version of Equation 4(b) from over 4000 reflection coefficient experimental test results. This can be generally expressed as:

$$K_r = tanh\, 0.16(\xi^{1.43}) \tag{5}$$

This equation extends the range of applicability to structure slopes with $1.5 \leq \cot\alpha \leq 4.0$ and $1.0 \leq \xi_{m-1,0} \leq 4.1$ with dimensionless crest freeboard of $0.58 \leq R_c/H_{m0} \leq 4.5$.

3. Material and Methods

3.1. Design of Model Tests

The Coastal Laboratory wave tank at Swansea University consists of an Armfield wave tank 30 metres in length, 0.8 metre in width and 1.2 metres in depth respectively. Waves are generated with a HR Wallingford computer-controlled piston paddle which has the capability to reproduce user-defined spectra of different types; includes a second-order wave correction due to Schäffer [20] and is also equipped with an active wave absorption system to minimize the wave reflection from the wave board. Each test was performed in this wave tank by applying an energy-conserved bimodal spectrum (Figure 2).

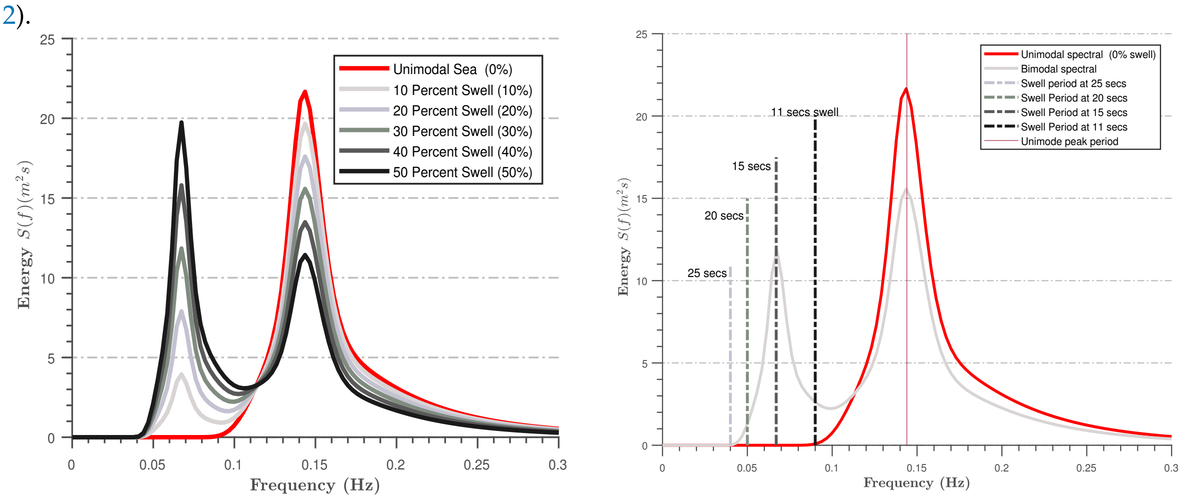

(a) *(b)*

Figure 2. *(a) An example of the bimodal spectra (b) Shifting patterns of swell peak periods from 11-25 secs [19].*

We refer to a sea state that has a fixed amount of energy but varying proportions of swell and wind sea as 'energy conserved' bimodal waves. The extremes of these conditions are 'pure wind sea'

 doi:10.20944/preprints202001.0061.v1

Peer-reviewed version available at *J. Mar. Sci. Eng.* **2020**, *8*, 133; doi:10.3390/jmse8020133

at one end and 'pure swell' at the other; with both cases resulting in a unimodal spectrum. For each test, sequences of 1000 random waves were generated.

Figure 3 shows the experimental set-up of an impermeable sloping seawall constructed of aluminium. The construction had a fixed 1:20 beach with a separate section that allowed seawalls of different slopes to inserted. Three different slope angles (Cot α = 1.5, 3, 0) were investigated at three different water levels. Detailed wave conditions and hydraulic parameters tested in this study are given in Table 1. A total of 823 bimodal wave conditions were tested to examine the influence of slope, swell peak periods and swell percentages on the reflection performances of the impermeable seawall. An array of four-wave gauges are positioned around the centre (with constant water depth) to capture both incident and reflected wave elevations effectively. As observed in Allsop & Hettiarachi [17], a wide range of frequencies can be obtained at central areas with constant water depth. The gauges are placed at central positions to meet the minimum requirements specified in Zelt & Skjelbreia [21]. The distances are computed using wavelengths computed from the dispersion relationship represented by individual wave conditions as $X_1 = 0$, $X_{12} = L/10$, $X_{13} = L/4$, $X_{14} = L/3$ as shown in the detailed experimental set up. Full details of the experiment can be found in [22,23].

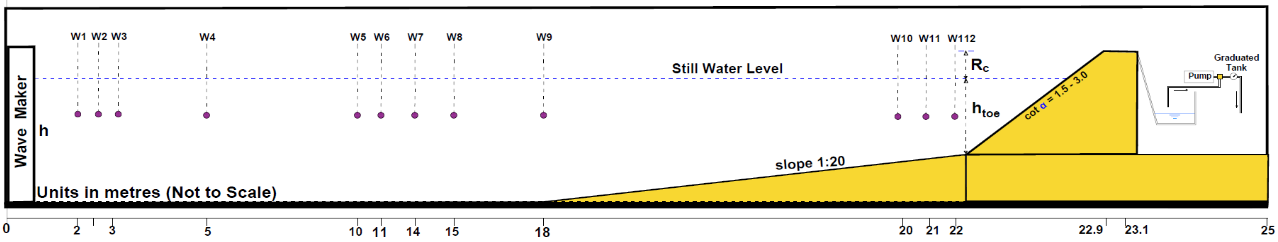

(a)

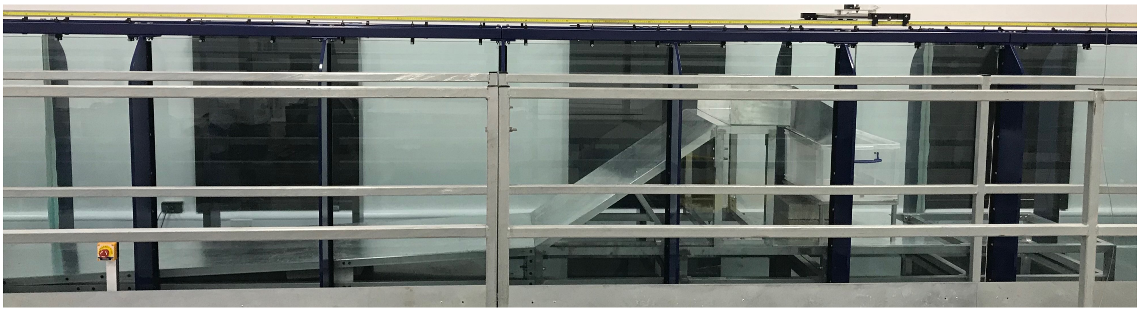

(b)

Figure 3. *(a) Layout of a schematic cross-section of the wave gauges applied for reflection analysis (b) Photograph of the constructed model*

3.2. Reflection Analysis

The reflection analysis of acquired signals was performed using the HR-Daq data acquisition and processing software that was incorporated with the wavemaker control system. This package separates reflected waves from the total signals using the method of Zelt & Skjelbreia [21]. The method is an extension of the three-wave gauges least-squares solution of reflection analysis first introduced by Mansard & Funke [24]. The wave signals were analysed using Fast Fourier Transform (FFT) into frequency components in the frequency domain. Some portions of wave elevation at earlier and later parts of each simulation were ignored to allow for consistency of wave elevations. The maximum length of discarded portions were 60 seconds at the begining and 120 seconds at the end. Bandpass filtering were applied to isolate the frequency band of $0.33f_p \leq f_p \leq 3f_p$.

Preprints (www.preprints.org) | NOT PEER-REVIEWED | Posted: 8 January 2020 doi:10.20944/preprints202001.0061.v1

Peer-reviewed version available at J. Mar. Sci. Eng. 2020, 8, 133; doi:10.3390/jmse8020133

Table 1. Bimodal wave conditions with Peak period of wind wave (T_{pW}), and Peak periods of swell wave T_{pS1-S4} tested in the present study.

Test No	H_{m0} (m)	T_{pW} (secs)	T_{pS1} (secs)	T_{pS2} (secs)	T_{pS3} (secs)	T_{pS4} (secs)	$h(m)$	$cot\alpha =$ 0.0	$cot\alpha =$ 1.5	$cot\alpha =$ 3.0	No of tests
T001	0.125	0.125	1.739	2.3712	3.162	3.953	0.7	0	1.5	3	13
T002	0.125	0.125	1.739	2.3712	3.162	3.953	0.7	0	1.5	3	13
T003	0.125	0.125	1.739	2.3712	3.162	3.953	0.7	0	1.5	3	13
T004	0.125	0.125	1.739	2.3712	3.162	3.953	0.7	0	1.5	3	13
T005	0.1	0.1	1.739	2.3712	3.162	3.953	0.65	0	1.5	3	13
T006	0.125	0.125	1.739	2.3712	3.162	3.953	0.65	0	1.5	3	13
T007	0.1	0.1	1.739	2.3712	3.162	3.953	0.65	0	1.5	3	13
T008	0.125	0.125	1.739	2.3712	3.162	3.953	0.65	0	1.5	3	13
T009	0.1	0.1	1.739	2.3712	3.162	3.953	0.6	0	1.5	3	13
T010	0.1	0.1	1.739	2.3712	3.162	3.953	0.6	0	1.5	3	13
T011	0.125	0.125	1.739	2.3712	3.162	3.953	0.6	0	1.5	3	13
T012	0.125	0.125	1.739	2.3712	3.162	3.953	0.6	0	1.5	3	13
T013	0.075	0.075	1.739	2.3712	3.162	3.953	0.65	0	1.5	3	13
T014	0.075	0.075	1.739	2.3712	3.162	3.953	0.65	0	1.5	3	13
T015	0.075	0.075	1.739	2.3712	3.162	3.953	0.65	0	1.5	3	13
T016	0.075	0.075	1.739	2.3712	3.162	3.953	0.65	0	1.5	3	13
T017	0.1	0.1	1.739	2.3712	3.162	3.953	0.7	0	1.5	3	13
T018	0.1	0.1	1.739	2.3712	3.162	3.953	0.7	0	1.5	3	13
T019	0.1	0.1	1.739	2.3712	3.162	3.953	0.7	0	1.5	3	13
T020	0.1	0.1	1.739	2.3712	3.162	3.953	0.7	0	1.5	3	13
T021	0.075	0.075	1.739	2.3712	3.162	3.953	0.6	0	1.5	3	13
T022	0.075	0.075	1.739	2.3712	3.162	3.953	0.6	0	1.5	3	13
T023	0.075	0.075	1.739	2.3712	3.162	3.953	0.6	0	1.5	3	13
T024	0.075	0.075	1.739	2.3712	3.162	3.953	0.6	0	1.5	3	13

The reflection analyses of Mansard & Funke and Zelt & Skjelbreia [21,24] apply strictly to linear waves. For the breaking wave cases, the non-linearity of the reflection performances cannot be accurately estimated by the method. The accuracy of Zelt & Skjelbreia method was determined using the flume without any structure. The free reflection characteristics of the open flume were used to calibrate the performance of the method of [21]. It was observed that the accuracy of the method was up to 90 percent. These adjustments are applied to all wave cases studied.

3.3. Estimation of reflection parameters

Some reflection parameters required for this study were estimated. These include the linear wave length, wave steepness and the dimensionless Iribarren number. Relationships obtained from these parameters are of special relevance to this study. The linear wave length $L_{m-1,0}$ applied here is calculated using the Newton-Raphson iteration technique on the dispersion relationship, (e.g. Reeve [25]).

$$L_{m-1,0} = \frac{gT_{m-1,0}}{2\pi} tanh\left(\frac{2\pi h}{L_{m-1,0}}\right) \tag{6}$$

Preprints (www.preprints.org) | NOT PEER-REVIEWED | Posted: 8 January 2020 doi:10.20944/preprints202001.0061.v1

Peer-reviewed version available at *J. Mar. Sci. Eng.* **2020**, *8*, 133; doi:10.3390/jmse8020133

In Eq. (6), h is the offshore water depth, and $T_{m-1,0}$ represents the spectral wave period. Also, the wave steepness $S_{m-1,0}$ can be defined in terms of the dimensionless ratio of the spectral wave height H_{m0} and the wave length $L_{m-1,0}$ obtained from Eq. (7):

$$S_{m-1,0} = \frac{H_{m0}}{Lm-1,0} \quad (7)$$

Similarly, the surf similarity parameter $\xi_{m-1,0}$ can be estimated from Eq. (8):

$$\xi_{m-1,0} = \frac{tan\alpha}{\sqrt{Sm-1,0}} \quad (8)$$

Other relevant parameters are the non-dimensional wave height H_{m0}/h and non-dimensional water depth $d/L_{m-1,0}$. Full details of equations solved to determine the reflection coefficient K_r are presented in Appendix 1. Table 1 presents the wave conditions tested in this study. As shown in the table for each Test numbers, for four different swell peak periods across three different sloping seawalls.

4. Results and Discussions

To derive a functional improvement to the reflection coefficient K_r of impermeable walls under bimodal sea conditions, effects of various secondary factors influencing K_r will be considered in this section. These factors includes the wall slope, water depth, wave steepness and the crest freeboard.

4.1. Influence of Wall Slope on Reflection Characteristics

Reflection characteristics of a coastal seawall can be determined by the steepness of the wall slope. Combined plots of the relationship between the reflection coefficient and the breaker index parameters are presented in Figure 4a–b. Figure 4(a) presented results for a unimodal sea states while reflection results due to bimodal sea states are represented in Figure 4(b). In general, for unimodal and bimodal sea conditions, K_r varies between 0.4 and 1.038. As expected, lower values of K_r are observed gentle slope of 1:3, while higher of K_r are clearly observed for the case of vertical seawall. These results are consistent with the findings of Seelig & Ahrens [10] and Allsop and Hettiarachi [17].

The range in K_r for a vertical wall depends largely on the degree of wave overtopping, and it increases as the crest freeboard increases. For sloped seawalls, the K_r is directly proportional to $\xi_{m-1,0}$ of the incident waves. In bimodal seas, higher bound of K_r is created which corresponds to swell of long period exhibited by the bimodal seas.

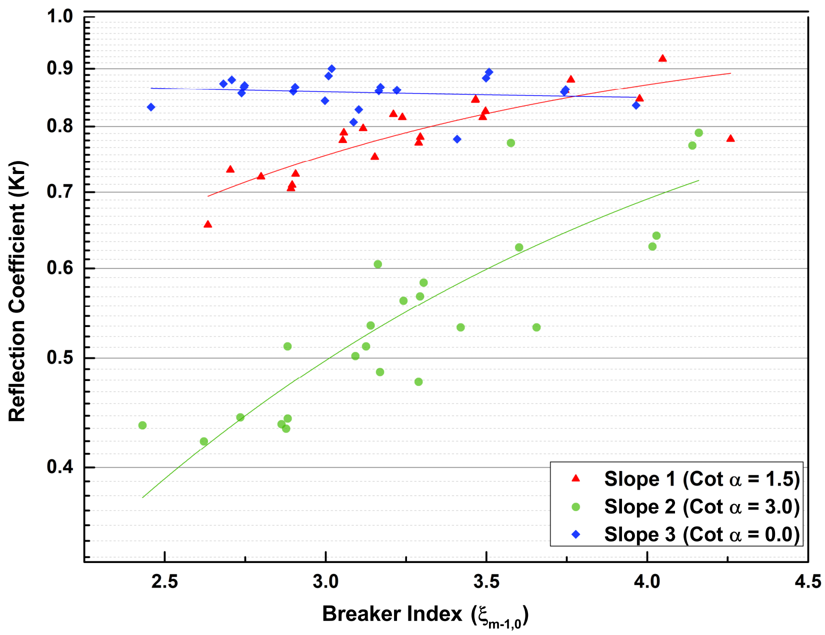

(a)

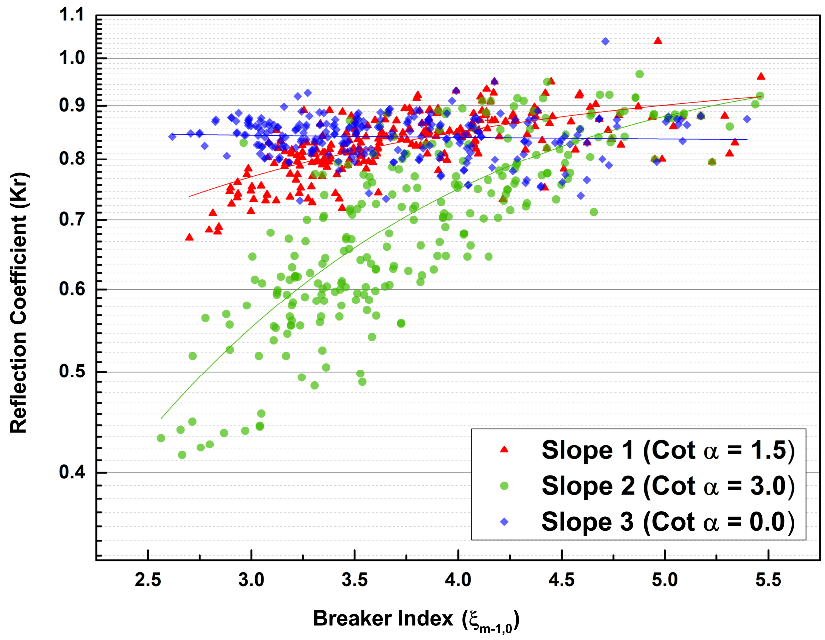

(b)

Figure 4. *Comparison of the reflection coefficient K_r and breaker parameters $\xi_{m-1,0}$ across three slopes (cot α = 1.5, 3.0 and 0.0) as shown under: (**a**) Unimodal sea states; (**b**) Bimodal sea conditions.*

Figure 5 shows a combined plot of the best-fit curves of K_r against $\xi_{m-1,0}$ for both unimodal (solid lines) and bimodal (in dotted lines) across different slopes are presented. It is obtained by applying the non-linear fit algorithm to all the datasets under unimodal and bimodal seas. Unimodal sea states exhibited similar trends as the bimodal sea conditions under the same test conditions. However, the relationship between K_r and $\xi_{m-1,0}$ are more extended in the bimodal sea states than in the unimodal sea conditions. It is the long periods in the bimodal seas that is responsible for this occurrence. As the wave period increases, there is a further reduction in wave steepness while values of $\xi_{m-1,0}$ increases.

Preprints (www.preprints.org) | NOT PEER-REVIEWED | Posted: 8 January 2020 doi:10.20944/preprints202001.0061.v1

Peer-reviewed version available at J. Mar. Sci. Eng. 2020, 8, 133; doi:10.3390/jmse8020133

It follows that values of K_r are inversely proportional to the wave steepness as reported in previous studies (for example, Seelig & Ahrens [10]).

Least reflections are observed for the gentle slope (cot α = 3.0), which is in accordance with the observations of van Gent, Neelamani & Sandya [18,26], and is a result of the wave energy dissipation.

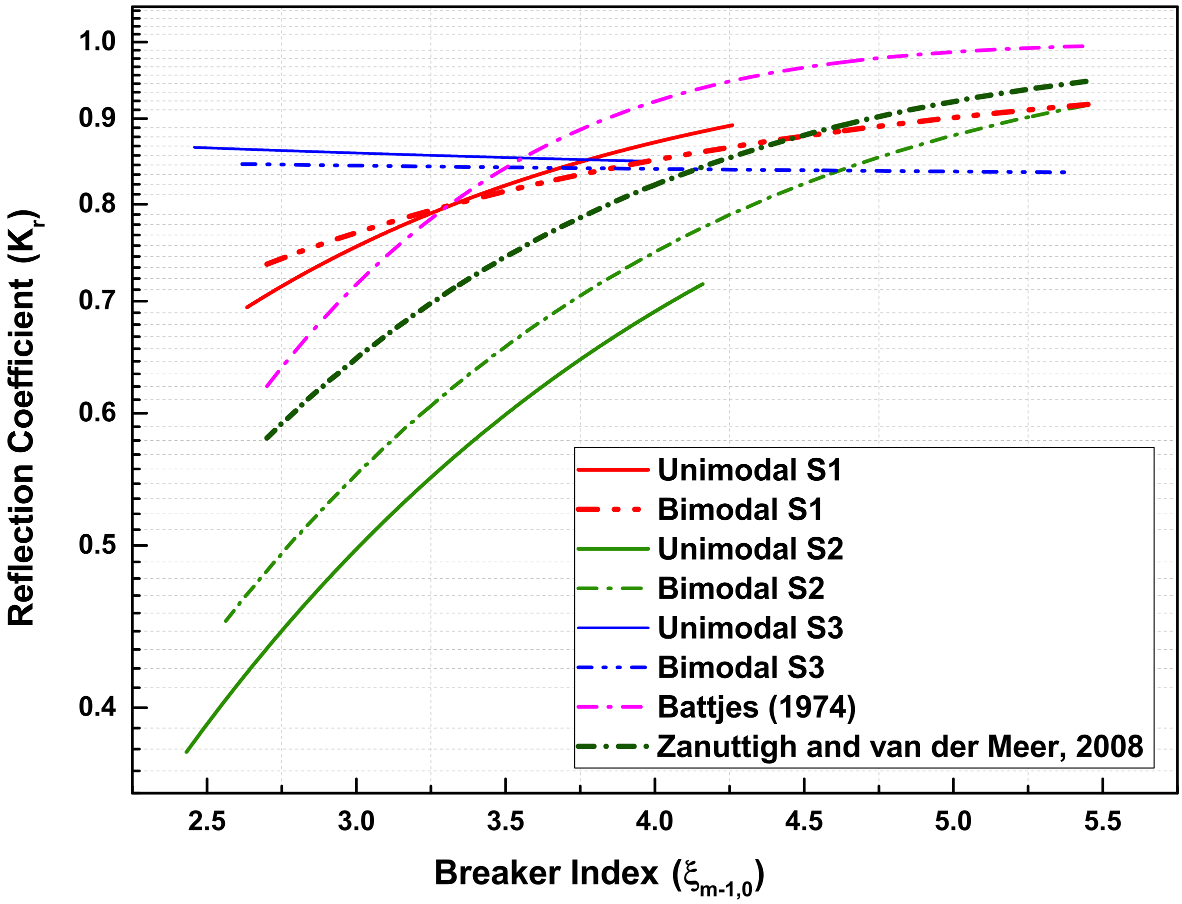

Figure 5. *Variations of reflection coefficient K_r with breaker index $\xi_{m-1,0}$ across three different slopes*

Further examination of these results shows that the relationships between K_r and $\xi_{m-1,0}$ for unimodal state obtained in this study are within the bounds of previous studies derived by Battjes [8] and that of Zanuttigh & van der Meer [2]. However, a better fit is obtained from the modified K_r formulation derived by Zanuttigh & van der Meer [2]. The fitted coefficients of [2] does not accurately fit for the relationship between K_r and $\xi_{m-1,0}$ in bimodal seas.

Preprints (www.preprints.org) | NOT PEER-REVIEWED | Posted: 8 January 2020 doi:10.20944/preprints202001.0061.v1

Peer-reviewed version available at J. Mar. Sci. Eng. 2020, 8, 133; doi:10.3390/jmse8020133

4.2. Influence of Water Depth Variations

In this section the influence of water depth, h/L, on reflection coefficient, K_r, was investigated across three slopes (i.e., cot $\alpha = 0.0$, cot $\alpha = 1.5$ and cot $\alpha = 3.0$). Figure 6 presents these results for all the datasets acquired during this study. Generally, for the steep (cot $\alpha = 1.5$) and the mild sloping (cot $\alpha = 3.0$) seawalls, it is found that the value of K_r decreases with increasing relative depth h/L. This behaviour agrees with the findings of Neelamani & Sandya [18] and Nassar & Negm [27]. These observations are peculiar to plunging wave breaking phenomena as previously described in cited literatures. For the vertical seawall, the reflection coefficient K_r is almost independent of water depth. This is expected because of the reflection of waves by vertical walls irrespective of the depth limiting values. Standing waves are formed during these tests, and more energy is reflected than for sloping walls. These observations are similar for both the unimodal and bimodal sea states.

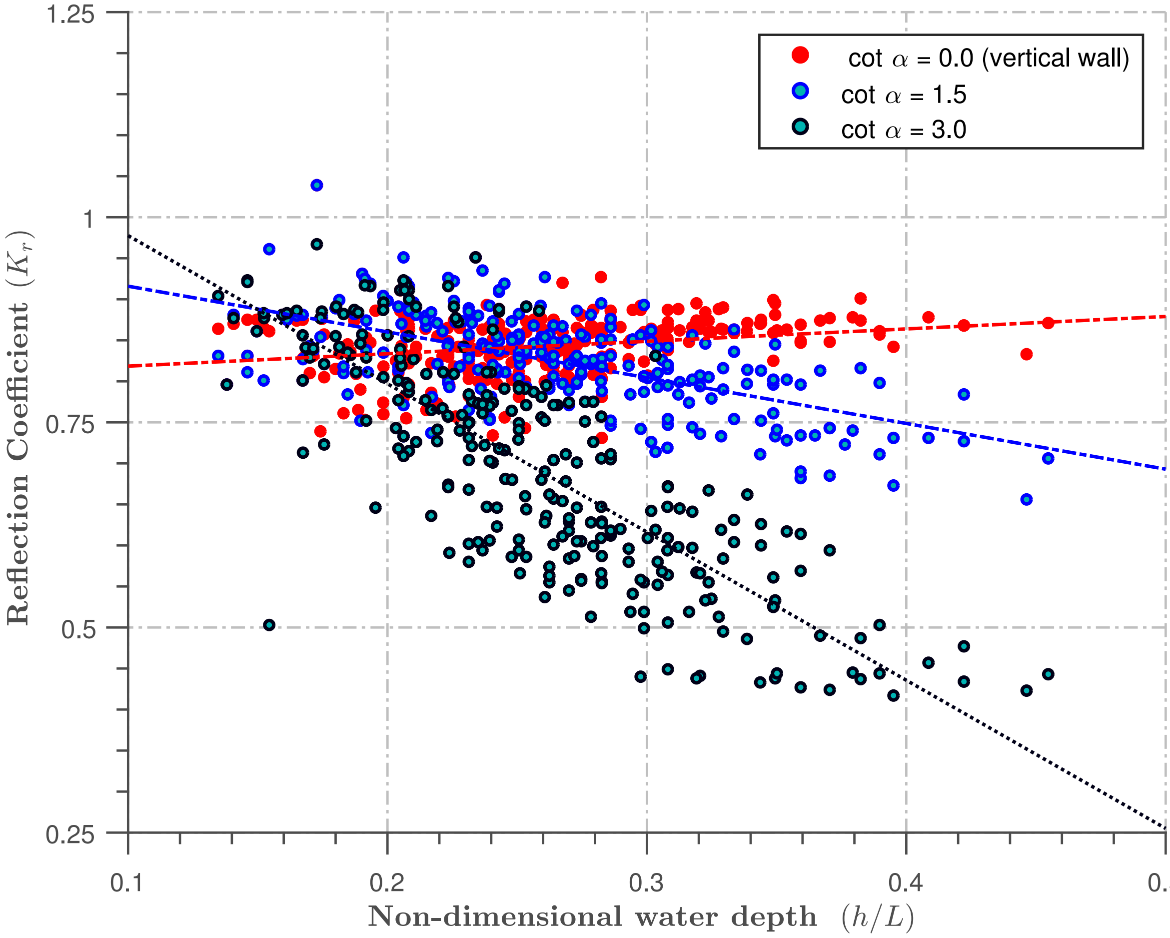

Figure 6. Variations of reflection coefficient K_r with non-dimensional water depth h/L across three different slopes investigated

Preprints (www.preprints.org) | NOT PEER-REVIEWED | Posted: 8 January 2020 doi:10.20944/preprints202001.0061.v1

Peer-reviewed version available at *J. Mar. Sci. Eng.* **2020**, *8*, 133; doi:10.3390/jmse8020133

4.3. Influence of Wave Steepness

Many sloping and vertical impermeable seawalls are built solely to dissipate wave energies that are directly incident on them. Reflected waves are produced whenever the waves are incident on the plain seawalls. In sloping seawalls, it has been suggested in Goda [28] that values of reflection coefficient K_r are inversely proportional to the incident wave steepness $S_{m-1,0}$. The suggestion is true for observations recorded in this study as shown in Figure (7). It forms completely similar correlation with the influence of water depth observed in previous section. However, the vertical seawall totally deviated from this theory in both cases.

The K_r performance of vertical seawall as shown in Figures (7-8) suggests that vertical seawalls would provide a more valuable protection to cities, harbours or ports as previously prescribed in previous studies for example

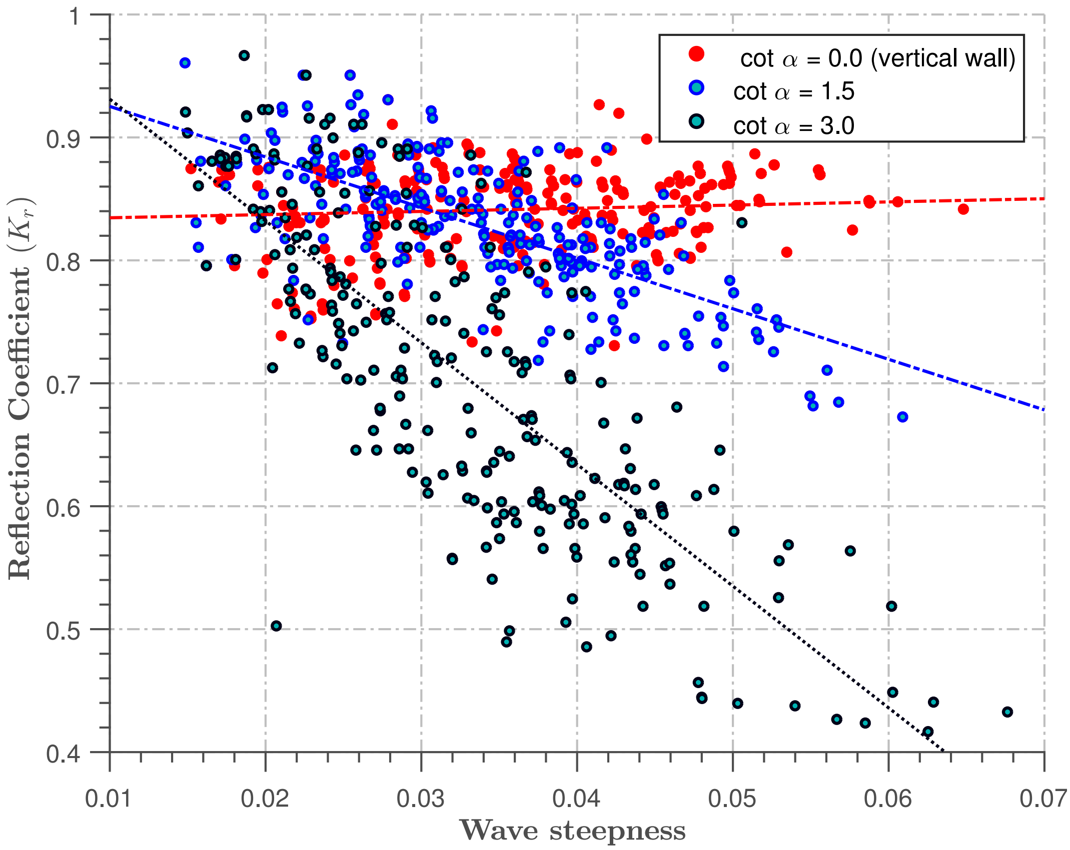

Figure 7. *Relationships between wave steepness and the reflection coefficient K_r across three different slopes investigated*

Preprints (www.preprints.org) | NOT PEER-REVIEWED | Posted: 8 January 2020 doi:10.20944/preprints202001.0061.v1

Peer-reviewed version available at J. Mar. Sci. Eng. 2020, 8, 133; doi:10.3390/jmse8020133

4.4. Effects of Crest Freeboard

Accurate selection of sizes of crest freeboard R_c/H_{m0} is an essential requirement for designing coastal seawalls against wave overtopping and to serve as flood barriers. Reliable prediction of reflection characteristics K_r of a coastal seawall suitable for selected R_c/H_{m0} is also key. In Figure 8, K_r is presented in terms of only R_c/H_{m0} across three seawall slopes. It can be seen that K_r is directly proportional to values of R_c/H_{m0}. As the crest freeboard increases, values of K_r also gradually increases. It implies that as crest freeboard reduces, there are more wave overtopping and tendencies for reflection reduces altogether.

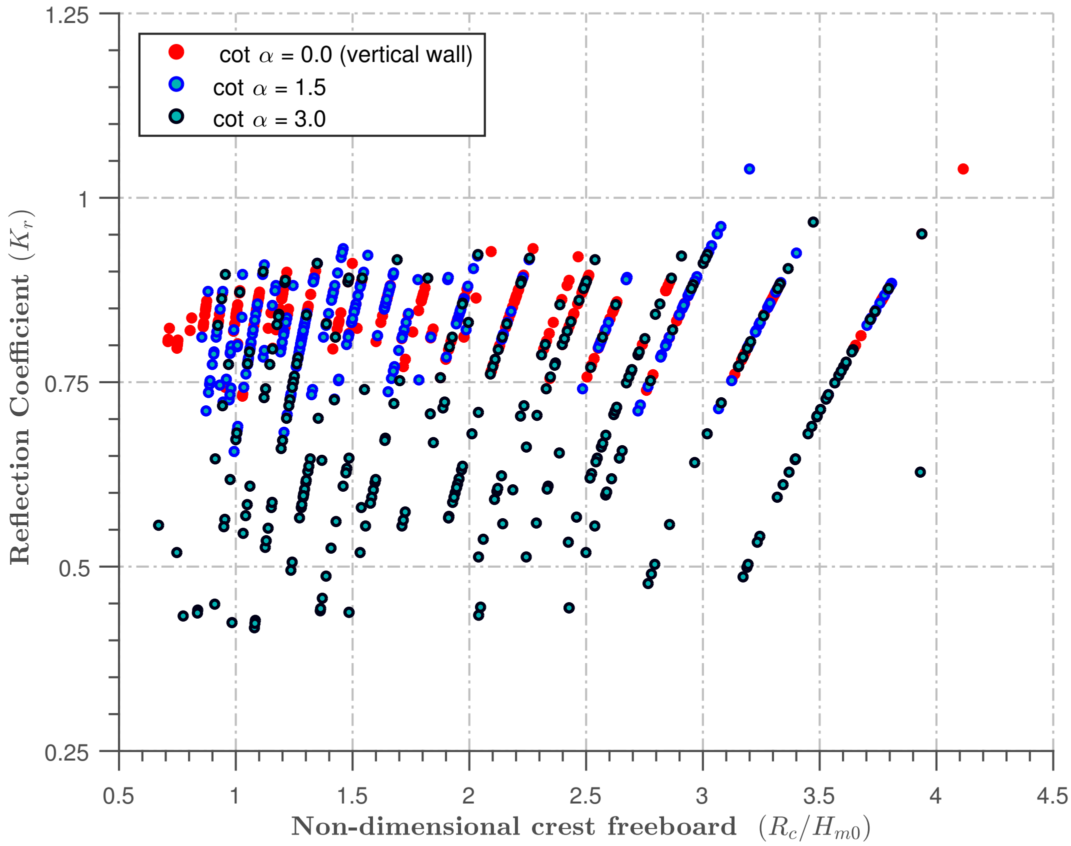

Figure 8. *Influence of dimensionless crest freeboard R_c/H_{m0} with the reflection coefficient K_r across three different slopes investigated*

 doi:10.20944/preprints202001.0061.v1

Peer-reviewed version available at J. Mar. Sci. Eng. 2020, 8, 133; doi:10.3390/jmse8020133

5. Reflection Coefficients of Steep Slopes Under Bimodal Waves

In order to establish an improved formulation for the reflection coefficient K_r for bimodal sea conditions, a more detailed analysis of the results were performed. Figure 9 presented a more detailed relationship obtained by performing non-linear regression analysis of the results between K_r and $\xi_{m-1,0}$ across each slope for the bimodal cases.

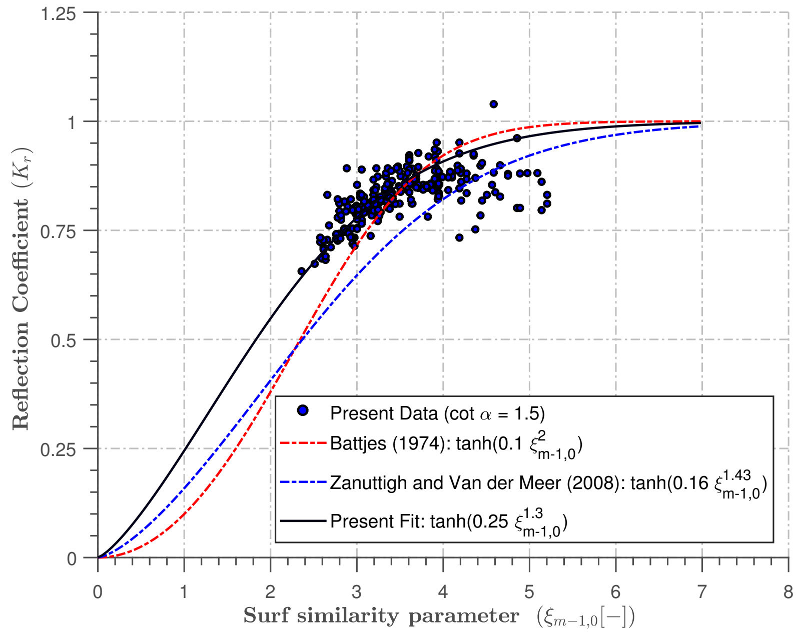

(a)

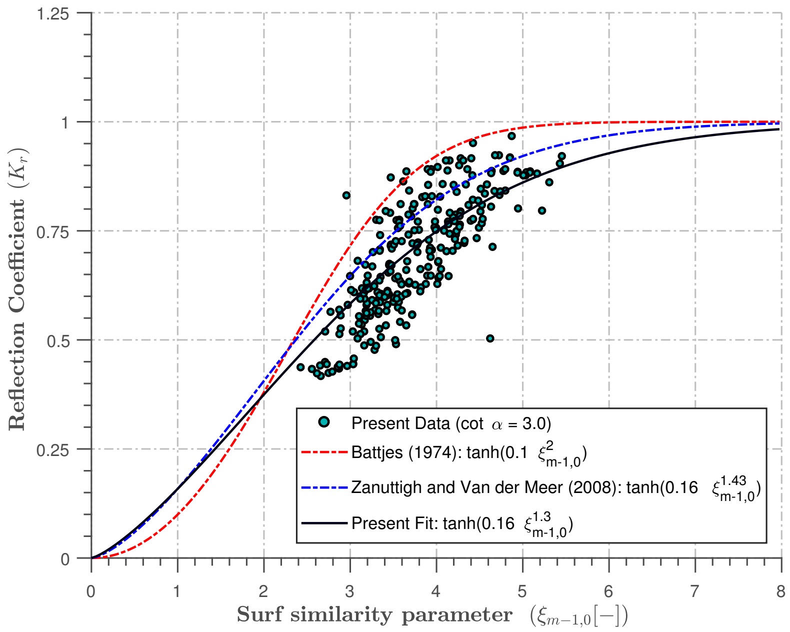

(b)

Figure 9. *A representation of the non-linear multi-regression fit between K_r and $\xi_{m-1,0}$ for sloping seawall with: (**a**) cot α = 1.5; (**b**) cot α = 3.0*

Based on multiple regression analysis of the observed datasets, predictive equation that considers effects of reflection due to bimodal waves are proposed. The equation contains two corresponding calibration coefficients applied in defining K_r of different impermeable slopes. It can only be applied for

Preprints (www.preprints.org) | NOT PEER-REVIEWED | Posted: 8 January 2020 doi:10.20944/preprints202001.0061.v1

Peer-reviewed version available at J. Mar. Sci. Eng. 2020, 8, 133; doi:10.3390/jmse8020133

sloping seawalls under bimodal sea conditions. The coefficients are slightly modified from Zanuttigh & van der Meer [2]. For simplicity, a more general form of Equation (5) can be written in terms of coefficients a and b presented in Equation (9):

$$K_r(a,b) = tanh\, a(\xi^b_{m-1,0}) \tag{9}$$

As a general rule of conditions for bimodal seas, values of a and b can be simplified:

$$\left.\begin{aligned} K_r &= tanh\left(a\xi^b_{m-1,0}\right) \\ \xi_{m-1,0} &= (2.4 \leq \xi_{m-1,0} \leq 5.5) \\ &\vdots \\ \frac{R_c}{H_{m0}} &= \left(0.8 \leq \frac{R_c}{H_{m0}} \leq 4.0\right) \end{aligned}\right\} \begin{aligned} &a = 0.25\,(for\ 1 \leq cot\alpha \leq 1.5) \\ &b = 1.3\,(Bimodal\ seas) \end{aligned} \tag{10}$$

$$\left.\begin{aligned} K_r &= tanh\left(a\xi^b_{m-1,0}\right) \\ \xi_{m-1,0} &= (2.4 \leq \xi_{m-1,0} \leq 5.5) \\ &\vdots \\ \frac{R_c}{H_{m0}} &= \left(0.8 \leq \frac{R_c}{H_{m0}} \leq 4.0\right) \end{aligned}\right\} \begin{aligned} &a = 0.16\,(for\ 1.5 \leq cot\alpha \leq 3.0) \\ &b = 1.3\,(Bimodal\ seas) \end{aligned} \tag{11}$$

To assess the suitability and conformance of the new formulation, a correllation assessment of the new equation with Zanuttigh & van der Meer [2] is made. Figure 10 shows a verification obtained in present study represented by Equations (10 & 11) and Equation (5) from the Zanuttigh & van der Meer [2]. The observed K_r and the predicted K_r are fully described in this figure for the two slopes ((**a**) cot α

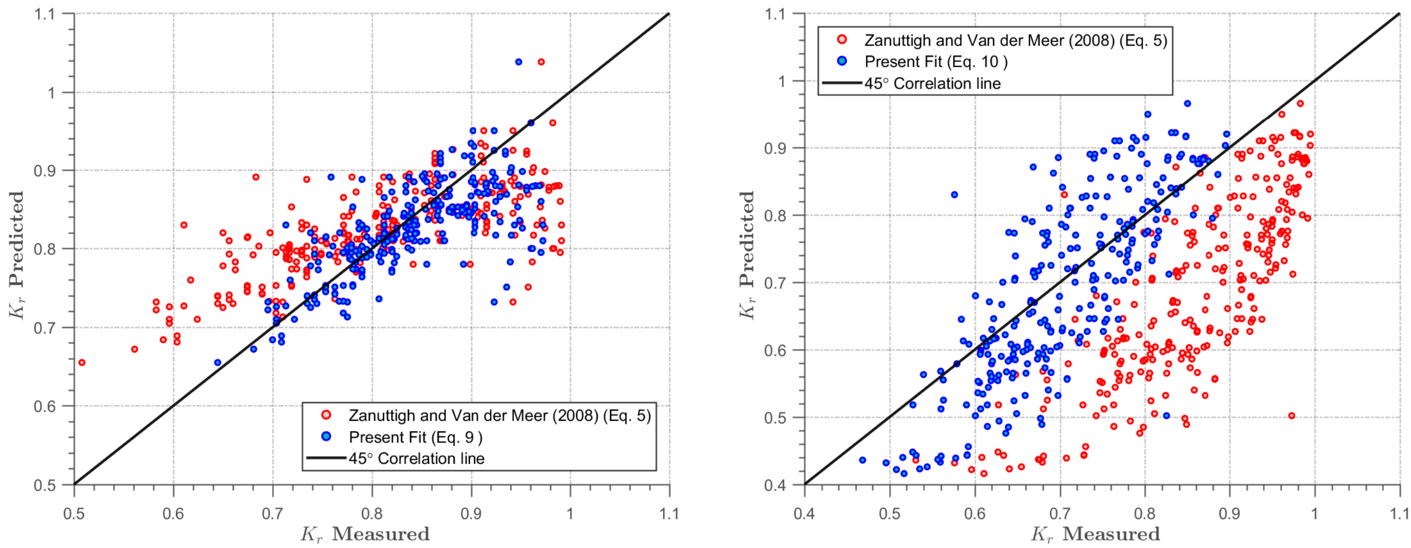

(a) *(b)*

Figure 10. *Comparison between the measured K_r and the predicted K_r of wave reflection coefficient (**a**) cot α = 1.5; and (**b**) cot α = 3.0*

Preprints (www.preprints.org) | NOT PEER-REVIEWED | Posted: 8 January 2020 doi:10.20944/preprints202001.0061.v1

Peer-reviewed version available at J. Mar. Sci. Eng. 2020, 8, 133; doi:10.3390/jmse8020133

As shown in these figures, observed data points are well distributed either side within 45^o correlation line. It can be deduced from the slight convergence of the agreement between observed and predicted values that Equation (10–11) works better in defining reflection characteristics of sloping seawalls under the influence bimodal waves than Equation (5). The prediction of prolonged breaker index imposed longer periods in swell waves are more accurately predicted with Equations (10–11) than Equation (5). It is under-predicting K_r under the bimodal cases most especially with increasing gentle slopes. The present formulation (Equations (10–11)) will be applicable at locations exposed to local storm waves and open oceans under bimodal wave conditions. Figure 11 expresses the appropriateness of the equation in predicting K_r under bimodal seas as represented in the residual plots described by the new formulations for both the steep slope (cot α = 1.5) and gentle slope (cot α = 3.0).

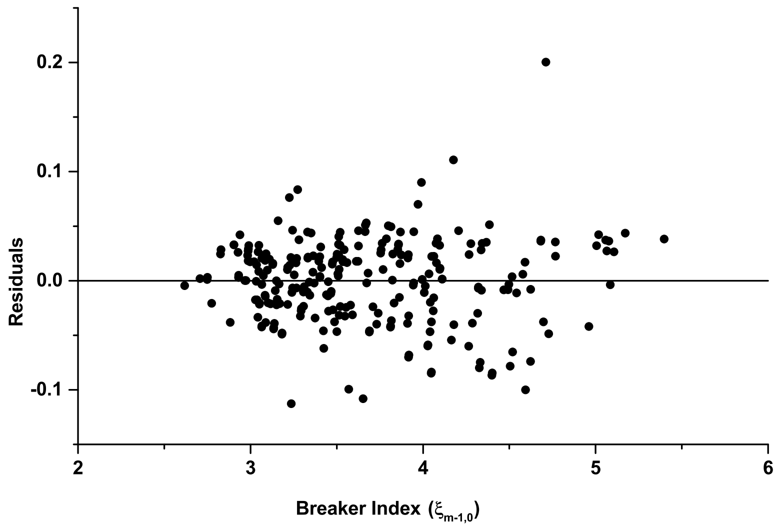

(a)

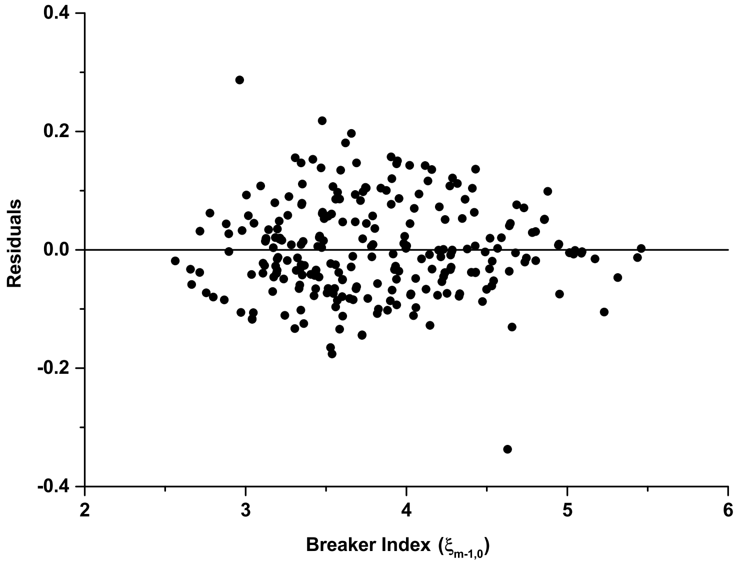

(b)

Figure 11. *Comparison between the measured K_r and the predicted K_r of wave reflection coefficient (**a**) cot α = 1.5; and (**b**) cot α = 3.0*

6. Conclusions

This study has examined the reflection performance of smooth sloping impermeable aluminium seawall under bimodal sea states. Three different sloping seawalls placed were investigated at three different water levels to conduct 823 successful storm tests. An array of four wave gauges positioned around the centre (with constant water depth) were applied to effectively capture both incident and reflected wave elevations. The Fast Fourier Transform (FFT) were applied to decompose analysed wave signals from four number wave gauges into frequency components in the frequency domain. The analysed reflection response of the studied coastal seawall is highly dependent on the seawall slope and wave bimodality. The resultant reflection coefficient also increases with swell peak periods and swell percentages. From the results of the reflection tests are presented and analysed in this paper yielding an improved empirical formula to determining reflection under bimodal sea conditions. New expressions for the reflection coefficient to take into account swell driven seas with wave bimodality have been proposed.

Author Contributions: S.O. conceived and wrote the paper draft. S.O. performed the experimental work simulations. H.K and D.E.R. contributed to the analysis and discussion of the results and also revised the paper.

Funding: This research was funded by The Petroleum Technology Trust Fund (PTDF), Nigeria (Grants No. OSS/PHD/842/16).

Acknowledgments: The author will like to acknowledge Dr. Jose Horrillo-Caraballo and Thomas van Veelen for great assistance while conducting the experimental tests. The author also acknowledge Professor Thomas Lykke Andersen and Professor Peter Frigaard for the generous workshop on generation and analysis of waves in physical models.

Conflicts of Interest: The authors declare no conflict of interest.

Abbreviations

The following abbreviations are used in this manuscript:

ξ	Breaker index or Surf similarity parameter
$\xi_{m-1,0}$	Breaker Index with L_o based on $S_{m-1,0} = H_{m-1,0}/L_{m-1,0}$
ξ_p	Breaker Index with L_p based on T_p
T_p	Peak period
FFT	Fast Fourier Transform
H	Wave height
IFFT	Inverse Fast Fourier Transform
H	Significant wave height
Jonswap	Joint North Sea Wave Project
K_r	Reflection coefficient
SSER	Sea-Swell energy ratio
T_{pS1-S4}	Peak periods of swell wave from 1 to 4
T_{pW}	Peak period of wind wave
UK	United kingdom
$S_{m-1,0}$	Wave Steepness derived from $T_{m-1,0}$
K_r	Reflection coefficient

References

1. Andersen, T.L.; Frigaard, P.; Burcharth, H.F. Lecture notes for the course in water wave mechanics **2014**.
2. Zanuttigh, B.; van Der Meer, J.W. ave reflection from coastal structures in design conditions. *Coastal Engineering* **2008**, *55*, 771 – 779. doi:doi:10.1016/j.coastaleng.2008.02.009.

3. Hawkes, P.J.; Coates, T.; Jones, R.J. Impacts of Bimodal Seas on Beaches, Hydraulic Research Wallingford. *HR Wallingford Report* **1998**, p. 80. doi:http://eprints.hrwallingford.co.uk/711/1/SR507.pdf.
4. Thompson, A.D.; Reeve, D.E.; Karunarathna, H. Modelling extreme wave overtopping at Aberystwyth Promenade. *Water* **2017**, p. 663.
5. Polidoro, A.; Pullen, T.; Eade, J. Gravel beach profile response allowing for bimodal sea states. *Proceedings of the Institution of Civil Engineers – Maritime Engineering* **2018**, *171*, 145 – 146. doi:https://doi.org/10.1680/jmaen.2018.11.
6. Miche, M. Le pouvoir reflêchissant des ouvrages maritimes exposés à l'action de la houl. *Ann. Ponts Chausées* **1951**, pp. 285 – 319.
7. Ursell, J.; Dean, R.G.; Yu, Y. Forced small amplitude water waves: a comparison of theory and experiment. *Journal of Fluid Mech.* **1960**, *7*, 33 – 52.
8. Battjes, J.A. Surf similarity. *Proc. 14th Conf. on Coastal Eng. ASCE* **1974**, pp. 460 – 480.
9. Iribarren, C.; Nogales, C. Protection des Ports. *XVIIth Int. Nav. Congress Section II* **1949**, *Comm. 4*, 31 – 80. doi:https://doi.org/10.1016/0378-3839(96)00012-9.
10. Seelig, W.N.; Ahrens, J.P. Estimation of Wave Reflection and Energy Dissipation Coefficients for Beaches, Revetments, and Breakwaters. *Technical Paper No. 81-1, US Army Corps of Engineers* **1981**, pp. 1 – 41.
11. Numata, A. Laboratory formulation for transmission and reflection at permeable breakwaters of artificial blocks. *Coastal Engineering in Japan* **1976**, *19*, 47–58.
12. Losada, M.A.; Gimenez-Curto, L.A. An approximation to the failure probability of maritime structures under a sea state. *Coastal Engineering* **1981**, *5*, 147–157.
13. Postma, G. Wave reflection from rock slopes under random wave attack. *MS thesis, Delft University of Technology, Department of Civil Engingineering* **1989**.
14. Davidson, M.; Bird, P.; Bullock, G.; Huntley, D. A new non-dimensional number for the analysis of wave reflection from rubble mound breakwaters. *Coastal Engineering* **1996**, *28*, 93 – 120. doi:https://doi.org/10.1016/0378-3839(96)00012-9.
15. Allsop, W.; Bruce, T.; Pearson, J.; Besley, P. Wave overtopping at vertical and steep seawalls. *Marine Engineering* **2005**, *158*, 103–114.
16. van der Meer, J.W. Conceptual design of rubble mound breakwaters. In *Advances In Coastal And Ocean Engineering: (Volume 1)*; World Scientific, 1995; pp. 221–315.
17. Allsop, N.; Hettiarachchi, S. Reflections from coastal structures. In *Coastal Engineering 1988*; 1989; pp. 782–794.
18. Neelamani, S.; Sandhya, N. Wave reflection, run-up, run-down and pressures on plane, dentated and serrated seawalls. *Coastal engineering journal* **2004**, *46*, 141–169.
19. Orimoloye, S.; Karunarathna, H.; Reeve, D.E. Effects of Swell on Wave Height Distribution of Energy-Conserved Bimodal Seas. *Journal of Marine Science and Engineering* **2019**, *7*, 79.
20. Schäffer, H.A. Second-order wavemaker theory for irregular waves. *Ocean Engineering* **1996**, *23*, 47–88.
21. Zelt, J.; Skjelbreia, J.E. Estimating incident and reflected wave fields using an arbitrary number of wave gauges. *Proccedings, 23rd ICCE, Venice* **1992**, pp. 777–788.
22. Orimoloye, S.; Horrillo-Caraballo, J.; Karunarathna, H.; Reeve, D.E. Wave overtopping under bimodal sea conditions. *Coastal Engineering (Under review)* **2019**.
23. Orimoloye, S.; Horrillo-Caraballo, J.; Karunarathna, H.; Reeve, D.E. Modelling wave overtopping of steep impermeable structures under bimodal sea conditions. *Proceedings of Coastal Structures, Hannover, Germany* **2019**.
24. Mansard, E.P.; Funke, E. The measurement of incident and reflected spectra using a least squares method. In *Coastal Engineering 1980*; 1980; pp. 154–172.
25. Reeve, D.; Chadwick, A.; Fleming, C. Coastal Engineering: Processes, Theory and Design Practice. *Spon, London, 518pp* **2015**.
26. van Gent, M.R. The modelling of wave action on and in coastal structures. *Coastal Engineering* **1994**, *22*, 311–339.
27. Nassar, K.; Negm, A. Determination of optimum wave reflection of seawalls via experimental modeling. Scour and Erosion: Proceedings of the 8th International Conference on Scour and Erosion (Oxford, UK, 12-15 September 2016), 2016, p. 255.

Peer-reviewed version available at *J. Mar. Sci. Eng.* **2020**, *8*, 133; doi:10.3390/jmse8020133

28. Goda, Y. *Random Seas and Design of Maritime Structures*; World Scientific Publishing Co. Pte. Ltd., 2010; p. 708.